DOI 10.1007/s11041-019-00436-9
*Metal Science and Heat Treatment*, Vol. 61, Nos. 7 – 8, November, 2019 (Russian Original Nos. 7 – 8, July – August, 2019)

# STRUCTURAL STEELS

UDC 669.18:669.14:539.4

# RELATION BETWEEN THE MICROSTRUCTURE OF COLD-RESISTANT STEEL 20GL AND SOME PARAMETERS OF THE MELTING PROCESS

**V. P. Ermakova,[1] V. G. Smirnova,[1] I. V. Nekrasov,[1] O. Yu. Sheshukov,[1, 2] L. A. Marshuk,[1] and V. S. Gulyakov[1]**

Translated from *Metallovedenie i Termicheskaya Obrabotka Metallov*, No. 7, pp. 3 – 9, July, 2019.

The microstructure, impact toughness and melting parameters of cold-resistant steel 20GL are studied. The impact toughness of the steel at negative temperature ($KCV^{-60}$) is shown to be affected the most by the size of the primary (natural) grains of the metal. The size of the natural grains is shown to be dependent on the content of oxygen and (to a less degree) of silicon. Introduction of an elevated amount of slag-forming materials and aluminum into liquid metal provides the required (at most 0.005 – 0.008 wt.%) content of oxygen and an impact toughness ($KCV^{-60}$) no less than 0.167 MJ/m$^2$. Influence of the nonmetallic inclusions, of the size of actual grains, and of the content of pearlitic phase on $KCV^{-60}$ in normalized steel has not been detected or was not obvious.

***Key words:*** cold-resistant steel, microstructure, grain size, nonmetallic phase, impact toughness at negative temperature ($KCV^{-60}$), parameters of melting in open-hearth furnace.

## INTRODUCTION

Cold-resistant steel 20GL including that melted by the open-hearth method is used for making vital parts of machines and mechanisms operating under the conditions of North. Cast steels possess coarse primary grains, and their refinement is a complicated problem. Massive cast parts are hard to be heat hardened, and their heat treatment is usually limited to normalizing. This makes it important to determine the conditions favorable for grain refinement.

In Russia, the open-hearth process is competitive enough due to availability of low-cost energy carriers. Therefore, in some cases, (scale of production, products range and steel quality) an open-hearth production may substitute the "electric furnace, ladle-furnace" complex, which makes further optimization of the open-hearth process a quite timely task.

Important factors responsible for the high enough level of mechanical properties of steel 20GL are the parameters of melting and casting of the steel, which are determined primarily by the chemical composition and the microstructure of the metal.

The mechanical properties of steel 20GL may be raised by different methods including optimization of the processes of melting, casting, out-of-furnace treatment, inoculation, improvement of the purity with respect to nonmetallic inclusions, etc. The effect of the melting parameters on the quality of the metal is known to be complex, and we should distinguish the most significant factors of the whole set in order to raise the mechanical properties of steel 20GL.

The aim of the present work was to determine the relation between the microstructure of cold-resistant steel 20GL and some parameters of the melting process influencing considerably the impact toughness at negative temperatures.

## METHODS OF STUDY

The steel studied was melted in 60-ton open-hearth furnaces with scrap-ore processing. Heats *1* and *2* were melted from pig iron (GOST 805) constituting about 40% burden, steel scrap (GOST 2787), iron-ore pellets (ZhRO, TU 0722-003-00186938–2004), slag-forming materials (lime-

[1] Institute of Metallurgy of the Ural Branch of the Russian Academy of Sciences, Ekaterinburg, Russia (e-mail: metallography@mail.ru).
[2] Ural Federal University after the First President of Russia B. N. Eltsyn, Ekaterinburg, Russia.

**TABLE 1.** Chemical Composition and Impact Toughness of Normalized Steel 20GL

| Heat | Time of taking of samples | Content of elements, wt.% | | | | | | | $KCV^{-60}$, MJ/m$^2$ |
|---|---|---|---|---|---|---|---|---|---|
| | | C | Mn | Si | Al | S | P | O | |
| *1* | Start of casting | 0.19 | 1.21 | 0.34 | 0.045 | 0.016 | 0.028 | 0.0145 | 0.12 |
| | End of casting | 0.19 | 1.20 | 0.33 | 0.041 | 0.015 | 0.028 | 0.0142 | 0.17 – 0.18 |
| *2* | Start of casting | 0.21 | 1.13 | 0.21 | 0.022 | 0.013 | 0.033 | 0.0065 | 0.18 – 0.31 |
| | End of casting | 0.21 | 1.13 | 0.22 | 0.023 | 0.013 | 0.034 | 0.0071 | 0.20 – 0.31 |

stone, TU 14-2R-361–2004), ZhRO and ferroalloys, i.e., ferrosilicon FS45 (GOST 1415), ferromanganese FMn78 (GOST 4755), and ferrosilicomanganese MnS17 (GOST 4756). During melting, the furnace was loaded with ZhRO, limestone and ferroalloys. The duration of blocking was 2 h 30 min for heat *1* and 2 h 50 min for heat *2* including the duration of pure boiling of the metal, which lasted for 55 min for both heats. The temperature of heat *1* before deoxidation and alloying was 1650°C; that of heat *2* was 1640°C. Preliminary deoxidation and alloying of the steel in the furnace after the boiling was conducted with ferroalloys FMn78, MnS17, FS45 and coke (TU 763-199-00190437–2004). For the final deoxidation and alloying in the ladle we used FS75, MnS17, aluminum AV87 (GOST 295) and coke. The temperature of the metal in the ladle after deoxidation and alloying was 1590°C for both heats. The metal was not subjected to out-of-furnace treatment.

Specimens with cross section $10 \times 10$ mm and length 55 mm for determining the impact toughness of the steel were cut in the longitudinal direction from samples taken at the start and at the end of the casting and normalized (heated to $920 \pm 10$°C, held for 1 h, and cooled in air). After the impact tests, the specimens were cut in the transverse direction to prepare microsections. For comparison, we conducted a metallographic analysis of not normalized samples of steel 20GL.

The metallographic study was performed with the help of a NEOPHOT-2 microscope and a Micromet-5103 microhardness meter equipped with a Thixomet Pro image analyzer providing panoramic imaging of the microstructure of the steel. The images with an area of 100 mm$^2$ were used to evaluate the initial grain size of the ferrite by measuring the maximum and minimum sizes of not equiaxed grains [1]. The form factor ($K_f$) was calculated from the ratio of these values. An initial (primary) grain was understood as a crystallized dendrite with Widmanstatten ferrite formed on its boundaries during transformation. To determine the content of the pearlite phase in the heat-treated steel we used a linear method based on the Cavalieri–Aker principle [1]. The gas content was determined using an ELTRA ONH-2000 gas analyzer. The tests for impact toughness KCV were preformed using an MK-15 pendulum impact machine at a temperature of –60°C.[3]

[3] The study was performed using the equipment of the "Ural-M" Collective Use Center.

## RESULTS AND DISCUSSION

In accordance with the OST 32.183–2001 Standard the composition of steel 20GL (in wt.%) includes 0.17 – 0.25 C, 1.1 – 1.4 Mn, 0.3 – 0.5 Si, 0.02 – 0.06 Al, at most 0.040 S, 0.040 P, 0.30 Cr, 0.30 Ni, 0.30 Cu. The impact toughness $KCV^{-60}$ is at most 0.167 MJ/m$^2$.

The chemical composition and the impact toughness of the steel after normalizing are given in Table 1.

The OST 32.183–2001 Standard does not stipulate the content of hydrogen in the metal. The chemical analysis of steel 20GL has shown (Table 1) that the content of oxygen in heat *2* with the higher level of impact toughness is about twice lower than in heat *1*. The residual content of aluminum in heat *2* is also twice lower. By the data of A. P. Gulyaev [2], an open-hearth steel should contain at most 0.005 – 0.008 wt.% oxygen. The aluminum content in both heats matches OST 32.183–2001, whereas the oxygen content in heat *1* (Table 1) exceeds the recommended value considerably [2]. In the opinion of the authors of [3] the content of oxygen in metal depends only on the final deoxidation behavior and on the residual concentrations of the deoxidizing elements. Speaking of the degree of deoxidation of the steel in both heats we should pay attention to the difference in the contents of the segregating admixtures including P, S, Si and O. Their total content is about 0.39 wt.% in heat *1* and about 0.27 wt.% in heat *2*. These admixtures widen actively the double-phase range of the crystallization. According of the data of [4], the wider the crystallization range, the more manifested is the segregation and the larger the size of the forming crystals (grains).

Table 2 presents the content of materials introduced during melting into steel 20GL; Table 2 presents the composition of the studied metal during melting in the open-hearth furnace and casting.

Comparison of the data of Tables 2 and 3 shows that the lower oxygen content in the ladle of heat *2* is a result of the higher content of the introduced aluminum (1.74 kg/ton against 1.24 kg/ton in heat *1* ). The lower content of residual aluminum and oxygen in heat *2* (Table 3) indicates more intense removal of the aluminum-containing inclusions from the liquid metal of this heat. The ladle of heat *2* contains more coke, which also participates in the deoxidation, lowers the oxidation of the metal and of the slag, and does not form additional nonmetallic inclusions. The mass of the metal in

**TABLE 2.** Content of Materials Introduced during Melting of Steel 20GL and Slag Composition at the End of the Process

| Parameter | Heat | |
|---|---|---|
| | *1* | *2* |
| Open-hearth furnace | | |
| Slag-forming burden materials (without metallic part), kg: | | |
| lime | 3950 | 5845 |
| ZhRO | 800 | 400 |
| ferroalloys* | 350 | 400 |
| Slag-forming materials introduced during melting, kg: | | |
| lime | 2000 | 2400 |
| ZhRO | 600 | 1200 |
| ferroalloys** | 1150 | 1130 |
| coke | 200 | 300 |
| Slag composition at the end of the process, wt.%: | | |
| FeO | 11.1 | 15.6 |
| CaO | 42.2 | 35.9 |
| $SiO_2$ | 15.9 | 12.9 |
| Slag basicity ($CaO/SiO_2$) | 2.7 | 2.8 |
| Ladle | | |
| Mass of metal, kg | 28,300 | 20,100 |
| Mass of introduced aluminum, kg | 35 | 35 |
| Mass of introduced ferrosilicon, kg | 50 | 60 |
| Mass of introduced ferrosilicomanganese, kg | 210 | 190 |
| Mass of introduced coke, kg | 100 | 150 |

* Heat *1*: FS45 — 100 kg; FMn78 — 150 kg; MnS17 — 100 kg; heat *2*: FS45 — 100 kg; FMn78 — 100 kg; MnS17 — 200 kg.

** Heat *1*: Fs65 — 250 kg; FMn78 — 350 kg; MnS17 — 550 kg; heat *2*: FS65 — 250 kg; FMn78 — 400 kg; MnS17 — 480 kg.

the ladle of heat *2* is about 30% lower (Table 2), and the mixing process is more active, which promotes floating of inclusions into the slag. This is very important, because the conditions sufficient for removal of oxide inclusions do not exist in the furnace but do exist in the ladle. In addition, the two heats differ in the silicon content, i.e., the content of the introduced ferrosilicomanganese in heat *2* is lower at the same content of ferrosilicon (Table 2).

The main inclusions in the heats are sulfides. It is known [5] that the type or the form of precipitation of sulfide inclusions in crystallization of the metal is determined by the degree of the deoxidation, i.e., the residual content of aluminum and oxygen. When the steel contains 0.02% oxygen, the metal acquires only globular sulfides (type I); at 0.01 – 0.02% oxygen the types of sulfides are I and II (film ones); when the oxygen content is below 0.01%, there are only type II sulfides [6]. Then the metal of heat *1* (0.0145% oxygen) should contain only inclusions of type II, while the metal of

**TABLE 3.** Composition of the Metal before Teeming from the Furnace and in the Ladle

| Heat | Content of elements, wt.% | | | | | | |
|---|---|---|---|---|---|---|---|
| | C | Mn | Si | Al | P | S | O |
| During melting of the burden | | | | | | | |
| *1* | 0.398 | 0.256 | 0.002 | – | 0.003 | 0.016 | 0.0139 |
| *2* | 0.241 | 0.270 | 0.007 | – | 0.004 | 0.012 | 0.0132 |
| Before teeming from the furnace | | | | | | | |
| *1* | 0.202 | 1.266 | 0.354 | – | 0.014 | 0.016 | 0.0141 |
| *2* | 0.208 | 1.174 | 0.224 | – | 0.021 | 0.011 | 0.0158 |
| In the ladle | | | | | | | |
| *1* | 0.200 | 1.220 | 0.410 | 0.015 | 0.041 | 0.018 | 0.0141 |
| *2* | 0.200 | 1.090 | 0.270 | 0.019 | 0.021 | 0.015 | 0.0076 |

heat *2* (0.006% oxygen) should contain only sulfides of type I. In fact, both heats chiefly contained sulfide inclusions of type II, which agrees with the data of [7]. If we consider only the aluminum content in the steel [8], the metal with 0.1 – 0.4% carbon, as in our case, should acquire sulfides of type III. In addition, the authors of [8] assume that the content of sulfur in the interdendrite regions exceeds substantially the concentration of oxygen due to the deep deoxidation of the metal with aluminum, which promotes precipitation of inclusions of types II and III.

In the not normalized samples of heat *1* the streaks of sulfide inclusions and the sulfide eutectic consist primarily of globular particles and short films (Fig. 1*a* and *b*). It can be seen in Fig. 1*c* and *d* that the sulfide eutectic is represented by particles of different shapes and is located on "islands" of ferrite phase. In their turn, these "islands" are located inside grains rather than on grain boundaries. Heat *2* is virtually similar to heat *1* where the morphology, the sizes, and the content of sulfide inclusions are concerned. The time when the samples inspected for sulfide inclusions are taken is also not important. Only some sulfide films in heat *1* have a size of up to 10 μm, and heat *2* does not bear sulfide inclusions longer than 4 – 6 μm. In the opinion of the authors of [6] a sulfide phase of any type may precipitate on boundaries of primary (initial) grains. Therefore, there is no need to speak of the harmful effect of the sulfide phase on the impact toughness of the steel, because it contains either quite few or none at all long films, and the streaks and the films of sulfide inclusions are located only inside grains.

Heat *1*, which contains an elevated amount of oxygen and has the lowest impact toughness (Table 2), contains an inconsiderable number of endogenic oxide inclusions with a size of at most 1 – 3 μm. It seems that the small oxide inclusions in this heat have been preserved due to weak boiling of the metal during melting and inconsiderable refining.

The microstructure of the not normalized steel is presented in Fig. 2. It can be seen that at the start of the teeming, heat *1* is "afflicted" with segregations of Widmanstatten fer-

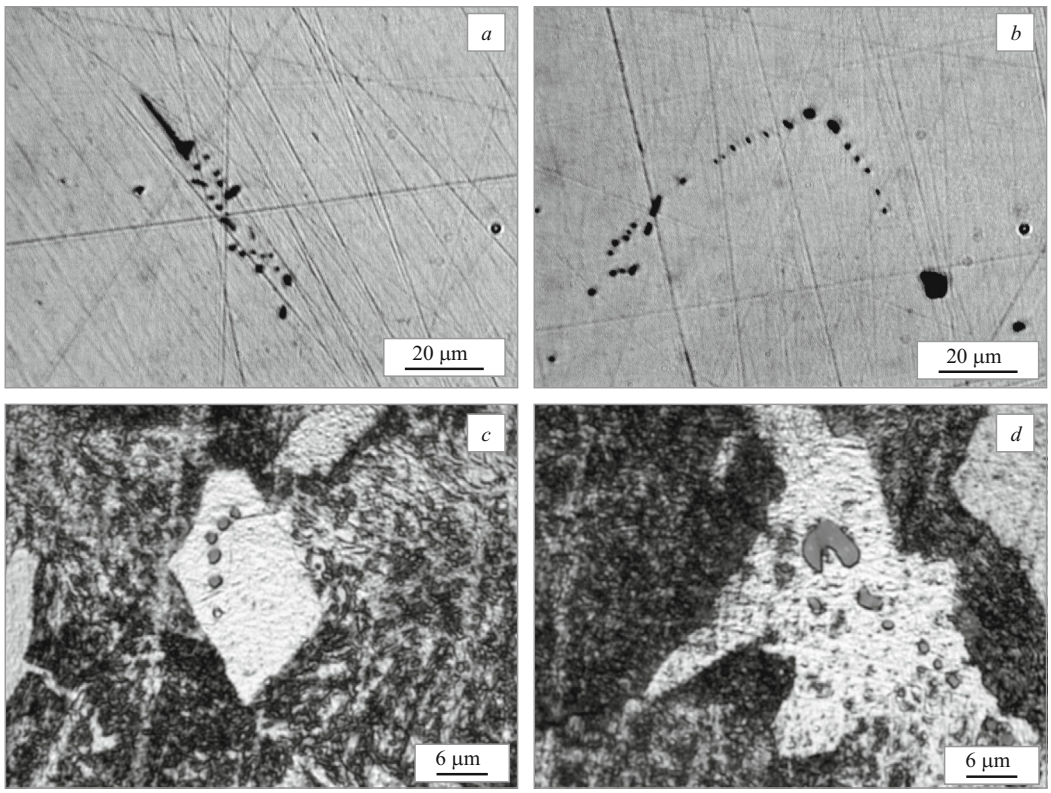


**Fig. 1.** Sulfide inclusions in samples of not normalized heat *1* of steel 20GL: *a*, *b* ) start and end of teeming, respectively (before etching); *c*, *d* ) start and end of teeming, respectively (after etching).

rite in the form of honeycomb formations inside grains (Fig. 2*a* ) and in the form of "brushes" of needles of Widmanstatten ferrite on grain boundaries (Fig. 2*b* ). In the end of the teeming, such large formations are absent, but small pieces of the broken "honeycomb" are still preserved (Fig. 2*c* ). Needles of Widmanstatten ferrite are still encountered in the samples taken in the end of the teeming, but they are noticeably thinner (Fig. 2*d* ).

The authors of [9] explain the formation of such structural abnormalities by strong segregation of silicon and manganese in the metal. In heat *1*, the content of silicon is 33 – 38% and that of manganese is 5 – 7% higher than in heat *2* (see Table 1). The microscopic chemical inhomogeneity of the austenite grains is the cause of nucleation of Widmanstatten ferrite at different times [9]. It should be noted that the critical temperature $A_3$ for heats *1* and *2* differs, i.e., it is 820°C for heat *2* and 860°C for heat *1* [10], i.e., the metal of heat *1* is in an austenitic condition for a longer time than that of heat *2*. We think that the factors mentioned explain the noticeably less number of Widmanstatten needles arranged dominantly on grain boundaries at the start of the teeming of heat *2* (Fig. 2*e* ). Honeycomb formations are absent, but we observe small groups or "cells" of Widmanstatten needles (Fig. 2*f* ). At the end of the teeming, the needles on the boundary look somewhat differently (Fig. 2*g* ) than at the start (Fig. 2*e* ), and the needle "cells" turn into individual needle fragments (Fig. 2*i* ).

In the opinion of the authors of [11, 12], Widmanstatten ferrite is responsible to a great degree for the low level of $KCV^{-60}$ of low-carbon steel 20GL. For the same reason, special attention is devoted to this anomalous phase in [13], where the authors determine the carbon content in the steel at which the appearance of Widmanstatten ferrite is possible and amend the temperature range (790 – 960°C) of the appearance of this anomalous phase during solidification of the low-carbon steel. On the contrary, it is stated in [14] that Widmanstatten ferrite may appear at a lower temperature, i.e., 690 – 620°C. According to the data of [15], Widmanstatten needles promote formation of pearlite grains of a complex wedge-like shape, which may affect the impact toughness more considerably than the Widmanstatten ferrite itself.

Figure 3 presents panoramic images of the microstructure of not normalized metal at the start and at the end of teeming.

The results of the measurement of the parameters of microstructure of the not normalized samples and their relations to the melting parameters are presented in Table 4.

It follows from Table 4 that the size of the primary (initial) grains in the not normalized steel is related to the level of the impact toughness after normalization. For this reason, we cannot agree with the inference of [16] that the impact toughness of the steel is affected only by the actual grain size, and the size of the primary ferrite grains is not important. The metal of heat *2*, where the primary grains are finer

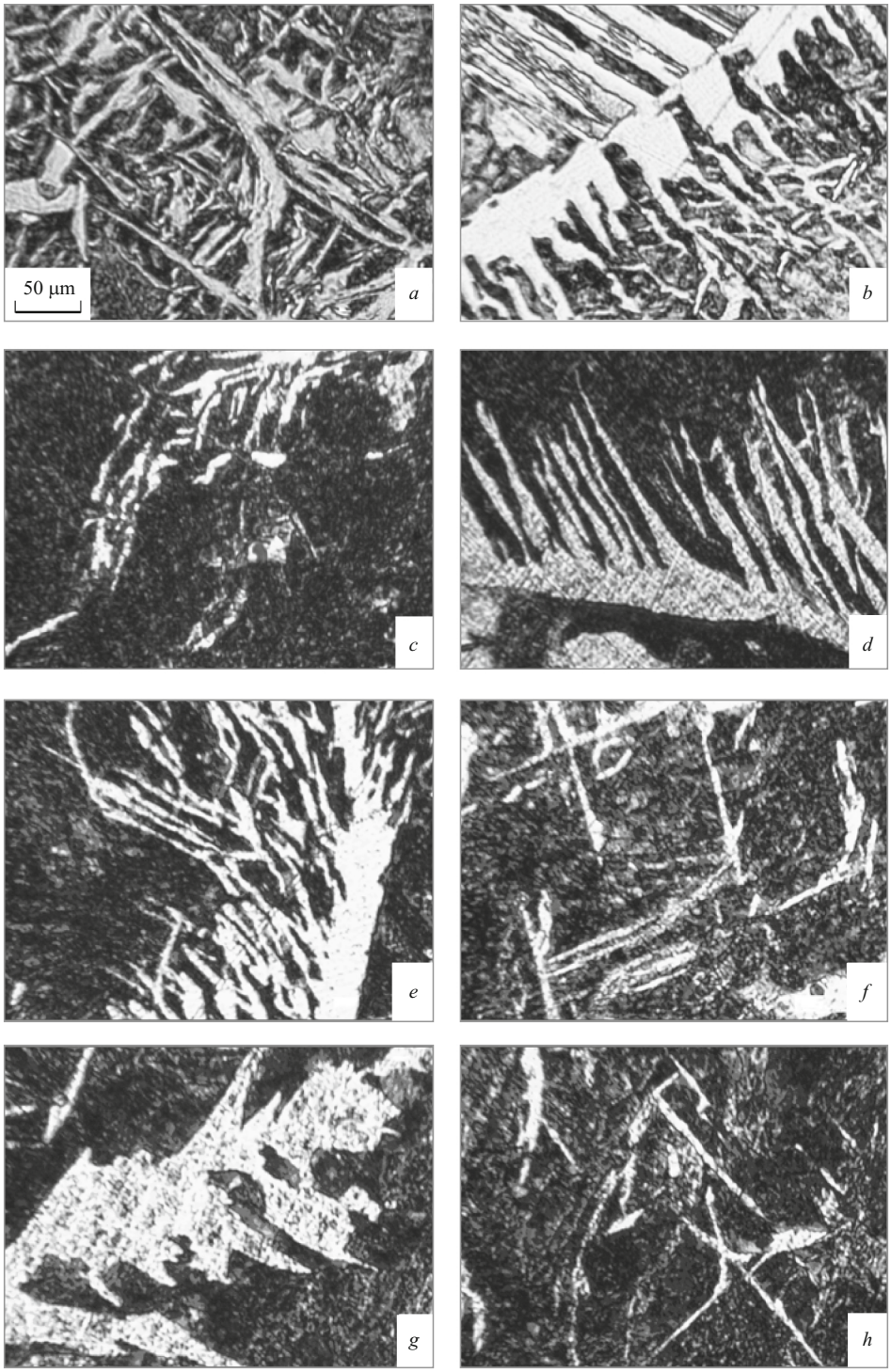


**Fig. 2.** Microstructure of not normalized heats *1* (*a* – *d* ) and *2* (*e* – *h* ) of steel 20 GL at the start (*a*, *b*, *e*, *f* ) and at the end (*c*, *d*, *g*, *h* ) of teeming.

(by 30 – 50%) and more equiaxed (the form factor is lower by 10 – 20%), has the highest impact toughness. In addition, the data of Table 4 show that the size of the primary gains in the samples taken from both heats at the end of teeming is lower and the impact toughness is higher than in the samples taken at the start of teeming. This is might be explainable by a difference in the temperatures at the start and at the end of the teeming, but we have no data on the temperature of the metal at the end of the teeming, because such measurement was technically impossible. According to the data of [17], in order to provide satisfactory filling of the casting mold, the temperature of the steel with composition in question should

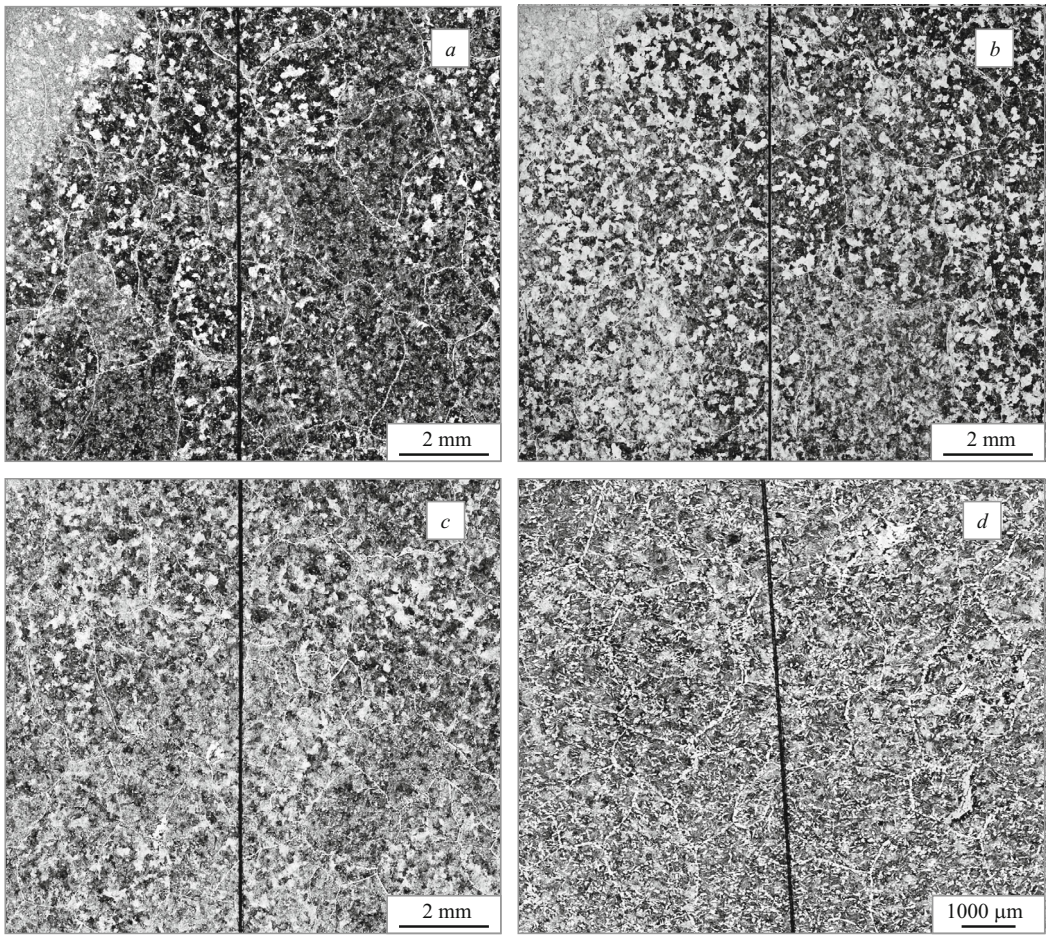


**Fig. 3.** Panoramic images of the microstructure of not normalized heats *1* and *2* at the start (*a*, *c*) and at the end (*b*, *d* ) of teeming.

exceed the liquidus temperature by no more than 30 – 60°C. Since the liquidus temperature of steel 20GL is 1513 – 1515°C, the teeming temperature should range within 1545 – 1575°C. It is possible that the temperature of the metal studied matched this temperature range at the end of the teeming.

Figure 4 presents the structure of the normalized heats. The recrystallization of the metal under normalizing has promoted removal of "brushes" and of the net of Widmanstatten ferrite over the boundaries of primary grains and formation of a ferrite-pearlite structure (Fig. 4*a* – *d* ). Single round-shape sulfides and elongated inclusions are arranged in the "bodies" of ferrite grains (Fig. 4*e* – *h* ). We have not detected sulfides on boundaries of ferrite grains with a rare exception when the sulfide particles adjoined or intersected grain boundaries. The elongated sulfide inclusions became globular under normalizing (Fig. 4*e* – *h* ). The results of our study do not coincide with the inference of [7], where it is stated that sulfides in the form of chains or a eutectic may be located only over boundaries of primary crystals.

**TABLE 4.** Effect of Some Melting Parameters on the Parameters of Primary (Initial) Grains in Not Normalized Steel and on the Impact Toughness of Normalized Steel 20GL

| Heat | Moment of sample taking | Temperature in ladle after teeming from furnace, °C | Characteristic of primary (initial) grains | | $KCV^{-60}$, MJ/m$^2$ |
|---|---|---|---|---|---|
| | | | Size over major axis/over minor axis, mm | Average form factor $K_f$ | |
| *1* | Start of teeming | 1590 | 2.2/1.3 | 1.69 | 0.12 |
| | End of teeming | – | 2.0/1.4 | 1.4 | 0.17 – 0.18 |
| *2* | Start of teeming | 1590 | 1.6/1.2 | 1.3 | 0.18 – 0.31 |
| | End of teeming | – | 1.4/1.1 | 1.3 | 0.20 – 0.31 |

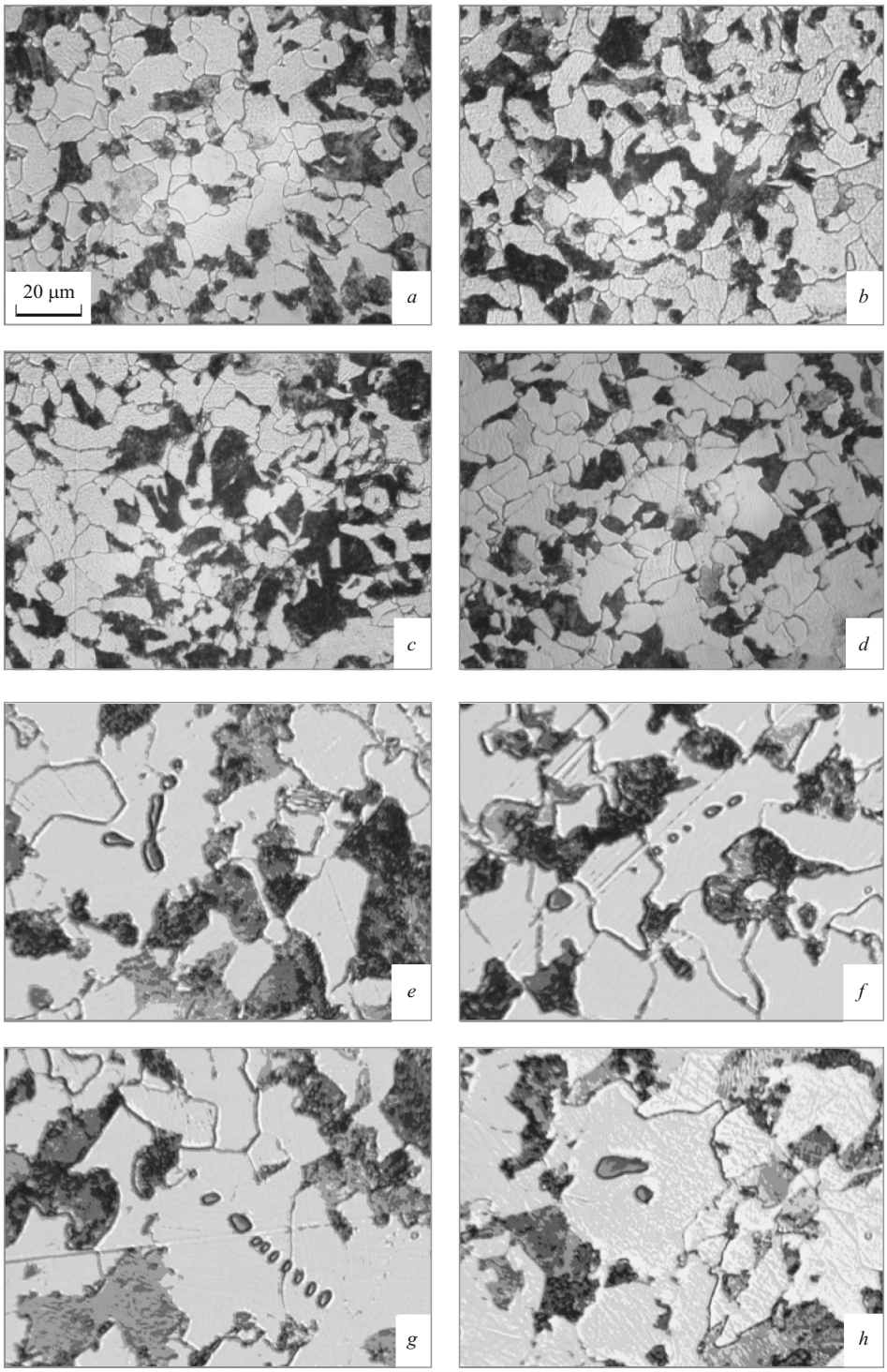


**Fig. 4.** Microstructure (*a* – *d* ) and sulfide inclusions (*e* – *h* ) in normalized heats *1* and *2* of steel 20GL at the start (*a*, *c*, *e*, *g* ) and at the end (*b*, *d*, *f*, *h* ) of teeming.

The results of the measurements of the parameters of microstructure of the heat-treated steel and their relation to some melting parameters are presented in Table 5.

It follows from Table 5 that, on the average, the metal of heat *1* contains more pearlite than that of heat *2*. In addition, the content of pearlite in the metal taken at the end of teeming of both heats is noticeably lower (Table 5). We have not explained yet the nature of this phenomenon, and its effect on the impact toughness is not obvious. We can see from the data presented that the average size of the actual ferrite grains at the end of teeming of heat *1* is considerably larger (the dominant grain size is No. 8) than at the start of the

**TABLE 5.** Effect of Some Melting Parameters on the Parameters of Microstructure and Impact Toughness of Normalized Steel 20GL

| Heat | Moment of sample taking | Temperature in ladle after teeming from furnace, °C | Microstructure and properties of cast samples after normalizing | | | |
|---|---|---|---|---|---|---|
| | | | Average size of actual ferrite grains, mm | Number of actual ferrite grains* (area, %) | Average content of pearlite, % | $KCV^{-60}$, MJ/m$^2$ |
| *1* | Start of teeming | 1590 | 0.013 | 10 (49%); 9 (36%); 8 (10%); 7 (5%) | 35 – 55 | 0.12 |
| | End of teeming | – | 0.016 | 8 (36%); 9 (26%); 10 (17%); 7 (11%) | 10 – 37 | 0.17 – 0.18 |
| *2* | Start of teeming | 1590 | 0.011 | 10 (50%); 9 (44%); 7 (6%) | 31 – 46 | 0.18 – 0.31 |
| | End of teeming | – | 0.013 | 10 (47%); 9 (38%); 8 (10%); 7 (5%) | 22 – 27 | 0.20 – 0.31 |

* According to the GOST 6539 Standard.

teeming, when the dominant grain size is finer (No. 10). However, the metal with large enough grains has an impact toughness of 0.17 – 0.18 MJ/m$^2$, which exceeds the value stipulated by OST 32.183–2001 (see Table 1). The metal of the same heat, which has finer grains at the start of teeming than at its end, exhibits a very low impact toughness (0.12 MJ/m$^2$ ). This proves that the impact toughness is primarily affected by the primary (initial) grains rather than by the actual grains.

## CONCLUSIONS

1. We have discovered a dominant effect of the size of primary (initial) grains on the impact toughness ($KCV$) of cold-resistant steel 20GL at negative temperatures.

2. The size of the initial grains is determined considerably by the content of oxygen and (to a less degree) of silicon, which widen the double-phase crystallization range and thus promote growth of the size of such grains.

3. Introduction of an elevated content of slag-forming materials and aluminum into the liquid metal promotes formation of the required content of oxygen (at most 0.005 – 0.008 wt.%) and an impact toughness ($KCV^{-60}$) of at least 0.167 MJ/m$^2$.

4. The influence of nonmetallic inclusions, of the size of the actual grains and of the content of the pearlite phase on $KCV^{-60}$ of the normalized steel has not been detected or is not obvious.

## REFERENCES


1. S. A. Saltykov, *Stereometric Metallography* [in Russian], Metallurgiya, Moscow (1970), 376 p.
2. A. P. Gulyaev, *Pure Steel* [in Russian], Metallurgiya, Moscow (1975), 184 p.
3. Yu. A. Shul'te, *Nonmetallic Inclusions in Electrical Steel* [in Russian], Metallurgiya, Moscow (1964), 207 p.
4. V. I. Yavoiskii, Yu. V. Kryakovskii, V. P. Grigor'ev, et al., *The Metallurgy of Steel* [in Russian], Metallurgiya, Moscow (1983), 584 p.
5. V. Dahl, H. Hengsterberg, and K. Duren, "Conditions of formation of sulfide inclusions of different types," *Chern. Metally*, No. 13, 17 – 27 (1966).
6. Ya. N. Malinochka and G. Z. Koval'chuk, *Sulfides in Steels and Cast Irons* [in Russian], Metallurgiya, Moscow (1988), 248 p.
7. H. Knuppel, *Deoxidation and Vacuum Treatment of Steel. Part 1. Thermodynamic and Kinetic Laws* [Russian translation], Metallurgiya, Moscow (1973), 312 p.
8. V. V. Lunev and V. V. Averin, *Sulfur and Phosphorus in Steel* [in Russian], Metallurgiya, Moscow (1988), 256 p.
9. V. A. Il'inskii, E. Yu. Karpova, L. V. Kostyleva, and N. I. Gabel'chenko, "Special features of the morphology and structure of Widmanstatten and polyhedral ferrite in low-carbon steels," *Izv. VolgGTU*, **4**(4), 154 – 158 (2010).
10. *The Physical Metallurgy and Heat Treatment of Steel and Cast Iron, A Handbook, Vol. 2. Structure of Steel and Cast Iron* [in Russian], Intermet Engineering, Moscow (2005), 528 p.
11. P. D. Odesskii and I. I. Vedyakov, *Low-carbon Steels for Metallic Structures* [in Russian], Intermet Engineering, Moscow (1999), 224 p.
12. E. Yu. Karpova, L. V. Kostyleva, and V. A. Il'inskii, "A study of tempering of Widmanstatten ferrite in the process of cooling of steel castings," *Metalloved. Term. Obrab. Met.*, No. 1, 20 – 23 (1998).
13. M. Durand-Charre, *Microstructure of Steels and Cast Irons*, Springer, Germany (2004), 404 p.
14. *The Metallography of Iron, Vol. II, The Structure of Steels* [Russian translation], Metallurgiya, Moscow (1972, 284 p.
15. V. A. Il'inskii, L. V. Kostyleva, and E. Yu. Karpova, "Special features of the structure and properties of cast low-carbon steels," *Metalloved. Term. Obrab. Met.*, No. 5, 2 – 4 (1995).
16. A. P. Gulyaev, *The Science of Metals* [in Russian], Metallurgiya, Moscow (1977), 647 p.
17. A. A. Filippenkov and V. M. Milyaev, *Steel Castings* [in Russian], UrO RAN, Ekaterinburg (2008), 266 p.